

FORCE ACTION OF A SHOCK WAVE ON A SOLID BODY

B. I. Zaslavskii,* V. R. Shlegel', S. Yu. Morozkin, and N. N. Denisov

UDC 533.6.011.72

Approximate engineering methods for determining the forces acting on solid bodies upon interaction with shock waves are proposed. These methods are verified experimentally with the use of a shock tube. The forces acting on bodies are measured by fast-response acceleration transducers. Good correspondence between measurement data and calculation results obtained by exact and approximate methods is observed.

1. Let a plane shock wave (SW) be incident on a body of arbitrary shape (Fig. 1). We introduce the coordinate system (x, y) in such a manner that the Ox axis coincides with the direction of SW propagation and the coordinate origin is located at the point where the shock-wave front contacts with the body (at any point on the contact line for a cylindrical body). The total surface force \mathbf{F} acting from the side of the flow on the surface of the body is given by

$$\mathbf{F} = - \oint_{S_m} p \mathbf{n} dS = F_x \mathbf{i} + F_y \mathbf{k} \quad \left(F_x = - \oint_{S_m} p n_x dS, \quad F_y = - \oint_{S_m} p n_y dS \right).$$

Here p is the pressure, $\mathbf{n} = (n_x, n_y)$ is the unit normal to the surface of the body, S_m is the area of the body surface, F_x and F_y are, respectively, the “drag” and “lifting” components of the force \mathbf{F} , and \mathbf{i} and \mathbf{k} are the unit vectors directed along the Ox and Oy axes, respectively. It is clear that $F_y = 0$ for bodies with a symmetry plane perpendicular to the plane of the shock wavefront.

In the problems of reflection of SWs of relatively low and moderate intensities from arbitrarily shaped bodies, the pressure behind the front of the reflected wave can be estimated by methods of the theory of geometrical acoustics, according to which the damping of shock and reflected waves is determined by the ratio between the cross-sectional areas of elementary ray tubes [1].

Let a reflected SW propagate in a gas with the initial pressure p_1 (p_1 is the pressure behind the front of the incident SW). The pressure $p_f(\mathbf{r})$ behind the element of the shock wavefront reflected from the point $\mathbf{r}_0 \in S_m$ and located at the point \mathbf{r} at the moment t is related to the pressure $p_f(\mathbf{r}_0)$ at the point \mathbf{r}_0 at the moment of reflection by the damping law [1]

$$p_f(\mathbf{r}) - p_1 = \left[\frac{R_1 R_2}{(R_1 + N_r t)(R_2 + N_r t)} \right]^{1/2} [p_f(\mathbf{r}_0) - p_1].$$

Here R_1 and R_2 are the principal radii of curvature of the reflected front at the point \mathbf{r}_0 , N_r is the velocity of the reflected SW in the coordinate system attached to the body, and the time t is reckoned from the moment of reflection. In the case where a plane acoustic SW reflects from a cylinder or sphere, this law yields the relation

$$\frac{p_f(\mathbf{r}) - p_1}{p_f(\mathbf{r}_0) - p_1} = \left(\frac{R_0}{R_0 + N_r t} \right)^\omega, \quad (1.1)$$

where R_0 is the radius of the cylinder or sphere. We have $\omega = 0.5$ for a cylinder and $\omega = 1$ for a sphere.

*Deceased.

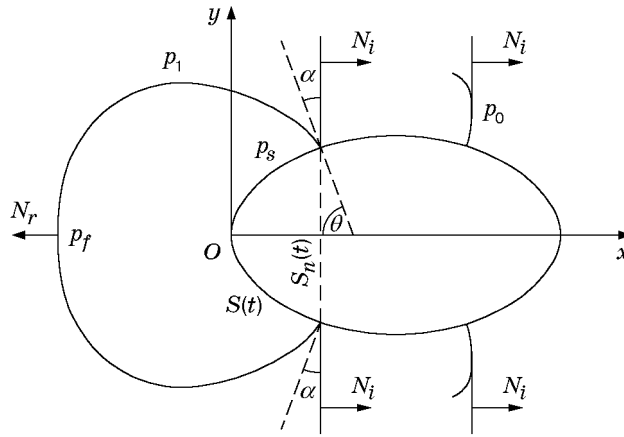


Fig. 1. Scheme of interaction between the shock wave and the solid body.

The laws of the form (1.1) can be used for more complex surfaces if a certain averaged (in the root-mean-square sense) radius is meant by R_0 , and the value of ω lies in the interval $0.1 \leq \omega \leq 1$. In the case of nonacoustic SWs where additional damping occurs, the value of ω must be increased. It was found that $\omega \approx 0.75$ for a cylindrical body [2], $\omega \approx 1.13$ for a spherical body, and $0.5 \leq \omega \leq 1.13$ for oblong bodies [3].

Bearing in mind the above-mentioned relations and assuming that $p_f = p_n$ at $t = 0$ (p_n is the pressure of the reflected SW upon "drag" reflection and the time t is reckoned from the moment the front of the incident SW contacts with the body), we describe the SW damping by the approximate formula

$$p_f - p_1 = \frac{p_n - p_1}{(1 + N_r t / R_0)^\omega}, \quad \left(p_n = p_1 \frac{(2\nu + 1)p_1 - \nu p_0}{p_0 + \nu p_1}, \quad \nu = \frac{\gamma - 1}{\gamma + 1} \right). \quad (1.2)$$

Here p_0 is the pressure ahead of the incident SW (pressure of unperturbed air) and γ is Poisson's adiabatic exponent.

We assume that, in the time interval considered, the averaged pressure on the reflecting surface is given by $p_S \approx p_f$ and, hence, the $p_S(t)$ variation is described by a formula similar to (1.2).

For a body in flow, the angle of incidence of the shock front on the solid surface varies continuously: $\alpha = \alpha(t)$ (Fig. 1). Depending on the angle of incidence, the regular and Mach regimes of reflection can occur [4]. The regular regime is realized for $\alpha > \alpha^*$, and the Mach regime for $\alpha < \alpha^*$, where $\alpha^* = \alpha^*(\Gamma_1)$ is the minimum angle at which regular reflection is still possible (the critical angle) [4] and $\Gamma_1 = (\rho_1 - \rho_0) / \rho_0$ (ρ_0 and ρ_1 are the densities of the gas ahead of and behind the front of the incident SW, respectively). The dependence $\alpha^*(\Gamma_1)$ is determined experimentally in [5, 6].

Zaslavskii and Safarov [6] showed that in the case of relatively weak SWs [$\varepsilon_1 = (p_1 - p_0) / (\gamma p_0) < 0.3-0.5$], the pressure drop at the reflecting surface is given by $p_S - p_0 \lesssim 2(p_1 - p_0)$ for $\alpha > \alpha^*$, the pressure p_S drops abruptly for $\alpha^*/2 < \alpha < \alpha^*$, and $p_S \approx p_1$ for $\alpha < \alpha^*/2$. It is noteworthy that, for $\alpha < \alpha^*$ in the case of Mach reflection beyond the midsection, the SW front is distorted upon SW diffraction to an extent that the front of a Mach or diffracted SW at the point of its intersection with the surface of the body remains perpendicular to this surface during the motion. Let t_r be the time it takes to reach the angle of incidence: $\alpha(t_r) = 2\alpha^*/3$. Since the length of the Mach SW is $L_M \ll R_0$ in the range $2\alpha^*/3 < \alpha < \alpha^*$, one can assume that the x coordinate of the line of intersection between the front and the surface $S(t)$ is determined from the formula $x = N_i t$ for $t < t_r$ and from the equation

$$t = t_r + \frac{1}{N_i} \int_{N_i t_r}^x \sqrt{1 + \left(\frac{dy}{dx} \right)^2} dx$$

for $t > t_r$. Here N_i is the velocity of the incident SW and $y = y(x)$ is the equation of the cross-sectional boundary of the body cut by the xOy plane.

The above relations allows one to determine approximately the pressure p_S and the force acting on the body \mathbf{F} by the following method. We divide the surface of the body in flow S_m into two regions: the region S_r which corresponds to the angles of incidence $2\alpha^*/3 < \alpha < \pi/2$, where regular reflection ($\alpha^* < \alpha < \pi/2$) and Mach reflection ($2\alpha^*/3 < \alpha < \alpha^*$) occur upon interaction of the SW with the body, and the region S_t , which

corresponds to the angles of incidence $-\pi/2 < \alpha < 2\alpha^*/3$, where Mach reflection ($0 < \alpha < 2\alpha^*/3$) and SW diffraction ($-\pi/2 < \alpha < 0$) occur.

We assume that the average pressure is determined by the formula

$$p_S = p_1 + \frac{p_n - p_1}{(1 + N_r t/R_0)^\omega}$$

on the surface S_r and it is given by $p_S = p_1$ on S_t . For $t < t_r$ (as long as the front interacts with S_r), the force F_x is given by formula

$$F_x = (p_S - p_0)S_n(t) = \left[p_1 + \frac{p_n - p_1}{(1 + N_r t/R_0)^\omega} - p_0 \right] S_n(t),$$

where $S_n(t)$ is the area of section of the body by a plane which passes through the line where the SW contacts with the surface of the body (Fig. 1). For $t_r < t < t \Big|_{\alpha=-\pi/2}$, we obtain

$$F_x = (p_1 - p_0)S_n(t) + \frac{p_n - p_1}{(1 + N_r t/R_0)^\omega} S_{nr},$$

where S_{nr} is the area of section of the body by a plane which passes through the boundary separating S_r from S_t .

Thus, when the shock front moves from the contact point, the ‘‘drag’’ force increases according to the following laws. Let $\theta = \pi/2 - \alpha$ (Fig. 1). Then,

$$F_x = \left[p_1 + \frac{p_n - p_1}{(1 + N_r t/R_0)^\omega} - p_0 \right] S_n(\theta), \quad x = R_0(1 - \cos \theta), \quad t = x/N_i \quad (1.3)$$

for $0 < \theta < \theta_r = \pi/2 - 2\alpha^*/3$ and

$$F_x = (p_1 - p_0)S_n(\theta) + \frac{p_n - p_1}{(1 + N_r t/R_0)^\omega} S_{nr}, \quad x = R_0(1 - \cos \theta), \quad t = t_r + \frac{R_0}{N_i} (\theta - \theta_r) \quad (1.4)$$

for $\theta_r < \theta < \pi$ (the angles are measured in radians). Here $S_n(\theta) = 2R_0 h \sin \theta$ for a cylinder of length h and $S_n(\theta) = \pi R_0^2 \sin^2 \theta$ for a sphere.

After the collapse of the shock front, the reflected front of the diffracted SW forms at the rear critical point, and the pressure in the diffracted front increases by twofold, which leads to the occurrence of the negative phase of force action.

In calculations, we used the dimensionless variables [7]

$$F_{xn} = F_x/(p_n - p_0)\sigma, \quad t_s = N_i t/R_0.$$

Here σ is the area of the body midsection perpendicular to the direction of SW propagation ($\sigma = 2R_0 h$ for a cylinder and $\sigma = \pi R_0^2$ for a sphere).

For a weak SW, we have $N_r \approx N_i$. In this case, formulas (1.3) and (1.4) written in the above-introduced dimensionless variables become

$$F_{xn} = \frac{1}{\sigma} \left[\frac{p_1 - p_0}{p_n - p_0} + \frac{p_n - p_1}{p_n - p_0} (1 + t_s)^{-\omega} \right] S_n(t_s) \quad (1.5)$$

for $0 < t_s < t_{sr} = 1 - \cos \theta_r$ and

$$F_{xn} = \frac{1}{\sigma} \left[\frac{p_1 - p_0}{p_n - p_0} S_n(t_s) + \frac{p_n - p_1}{p_n - p_0} (1 + t_s)^{-\omega} S_{nr} \right] \quad (1.6)$$

for $t_{sr} < t_s < t_s \Big|_{\theta=\pi} = t_{sr} + \pi - \theta_r$.

2. Experiments were performed with the use of a UT-4 setup consisted of a shock tube, the means of visualization and photographing of the wave pattern, the means of measuring forces, pressures, and time intervals, and the means of automatization of experiment and data processing.

A single-staged diaphragmed shock tube with a 85×125 mm rectangular cross section allowed us to generate SWs with relative intensities $0.05 < \varepsilon_1 < 0.7$.

Visualization was performed by the schlieren method by means of an optical knife in the focus of a Toepler device. As light sources, flash lamps were used. Photographing was performed by a waiting time magnifier (the exposure speed is up to $8 \cdot 10^6$ frames/sec) or a camera.

The SW parameters were measured by piezoelectric pressure gauges located in the walls of a low-pressure chamber and by a time-interval counter.

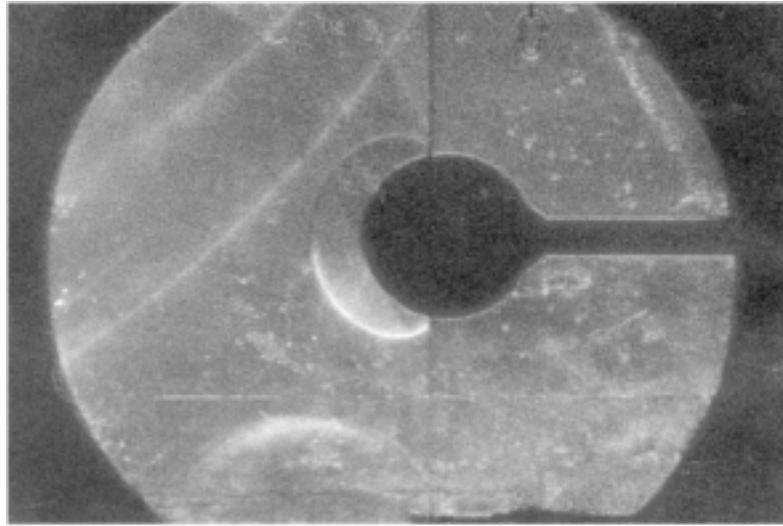


Fig. 2. Toeplerogram of a SW flow around a sphere (Mach-reflection regime).

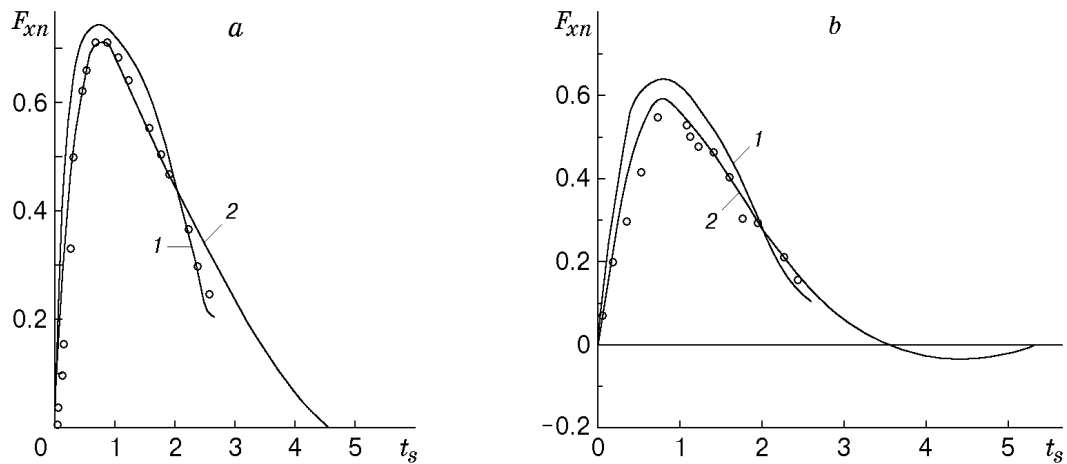


Fig. 3. The force F_{xn} versus time for a SW flow around a cylinder (a) and a sphere (b): curves 1 refer to approximate calculation by formulas (1.5) and (1.6), curves 2 to exact calculation [7], and points to experiment.

The forces acting on bodies were measured by piezoelectric gauges with an inert mass (accelerometers). The accelerometer comprised sensors (piezoelectric disks) located between the case (base) of the transducer and the relatively large inert mass.

The models to be tested were made of a steel in which the velocity of sound (approximately 5700 m/sec) is more than one order of magnitude greater than the SW velocity (350–430 m/sec). This allowed us to avoid measurement errors determined by the finite velocity of sound in the material of the model.

After amplification, the signals from the gauges were applied to storage oscilloscopes which were also high-rate analog-to-digital converters. For final processing, the signals from the oscilloscopes were introduced to a “Neuron” computer, and the SW and force-vector component parameters were calculated.

The signals from the accelerometers and pressure gauges were subjected to digital and analog processing. Digital processing was performed with the use of a special program on a “Neuron” computer. An information needed to determine the force acting on the body (signals from gauges, calibrations of the gauges, and the model and ambient-atmosphere parameters) was loaded into the computer. For analog processing of the signals, low-frequency filters with a cut-off frequency of 25 kHz were used. These filters allowed us to suppress completely the noise caused by excitation of the resonance frequencies of the accelerometers in the range 50–100 kHz.

3. Using an UT-4 setup, we studied experimentally the action of an SW on solid bodies. Experiments were performed for a cylinder (the cylinder axis was parallel to the SW front) and a sphere.

Figure 2 shows a photograph of the flow around the sphere visualized by the Toepler device.

Figure 3 shows the dimensionless forces F_{xn} acting on the cylinder (the length $h = 60$ mm and the radius $R_0 = 22.5$ mm) and the sphere versus the dimensionless time t_s for the relative SW intensity $\varepsilon_1 = 0.24$ ($\alpha^* = 0.7$ rad). Curves 1 were calculated by formulas (1.5) and (1.6). For the cylinder and the sphere, the range of the angles of incidence $2\alpha^*/3 < \alpha < \pi/2$ corresponds to the angles $0 < \theta < 1/12$ rad (see Fig. 1) and the coordinate $0 < x/R_0 < 0.57$. Curves 2 refer to the exact numerical calculation [7]. The calculation results obtained from formulas (1.5) and (1.6) agree well with exact numerical results [7] and experimental data, which supports the validity of the initial assumptions used in the derivation of these formulas.

REFERENCES

1. F. Friedlander, *Sound Pulses*, Cambridge (1958).
2. L. D. Landau and E. M. Lifshitz, *Hydrodynamics* [in Russian], Nauka, Moscow (1986).
3. R. H. Cole, *Underwater Explosions*, Dover, New York (1965).
4. R. Courant and K. D. Friedrichs, *Supersonic Flow and Shock Waves*, Interscience, New York (1948).
5. W. Bleakney and A. H. Taub, "Interaction of shock waves," *Rev. Modern Phys.* **21**, No. 4, 584–605 (1949).
6. B. I. Zaslavskii and R. A. Safarov, "Similarity of flows occurring upon reflection of weak shock waves from a rigid wall and a free surface," *Fiz. Goreniya Vzryva*, **9**, No. 4, 579–585 (1973).
7. V. N. Lyakhov, V. V. Podlubnyi, and V. V. Titarenko, *Action of Shock Waves and Jets on Structural Members* [in Russian], Mashinostroenie, Moscow (1989).